Radar Image Simulation and its Application in Image Analysis

G. Domik, F. Leberl
Research Center Graz and
Technical University Graz
Austria

M. Kobrick
Jet Propulsion Laboratory
Pasadena, USA

Commission III

Abstract

A system for simulating radar images was developed and so far applied in the fields of stereo viewability evaluation, radar image rectification and backscatter analysis. Emphasis in the simulation is on the correct geometric representation and on flexible input parameters. Variable input parameters are sensor configuration, imaging parameters and backscatter curves or look up tables to assign grey values to the image coordinates. Results from this analysis have been obtained from both optically and digitally processed data.

Introduction

Radar image simulation may serve to take the place of real images where big data sets are required (Kaupp et al.,1982; Domik et al. 1983a), to better understand imaging principles (Holtzman et al., 1978) and to help analyzing the real radar data (Domik et al., 1983b).

Radar images exhibit a dominating sensitivity to topographic slope. Therefore an analysis of the images depends on the correct understanding of topographic effects. Because radar is an imaging concept without analogos in the human senses it is of particular interest to support this understanding by image simulation.

Examples of previous simulation systems are by Holtzman et al., (1978) and Kaupp et al. (1982). The simulation discussed here emphasizes the correct image geometry and uses homogenous backscatter curves to model the radiometry as a function of the incidence angle.

Radar Image Simulation

The task of image simulation consists of two separate components -- a geometric one vs. a radiometric one. The geometric part of the simulation relates the object and image point. The radiometric task assigns grey values to each image pixel according to the properties of the corresponding object cell and an additional backscatter curve.

(a) Geometric Imaging Model

Two types of algorithms may be applied to establish the relationship between object and image point addresses. The straight forward approach is to start in the object space (the digital elevation model, DEM) and map the object space coordinates (DEM grid points) into the image plane by applying the radar equation; in its simplest form this is:

$$r^2 = (H - h)^2 + d^2$$

where:

- r ... slant range
- d ... distance between nadir and point to be imaged
- H ... flight altitude
- h ... height of imaged point

This results in non-equidistant grid points in the image as image space coordinates. Some sort of interpolation has to be applied to create a regularly spaced output.

The other approach to image simulation would be an image space algorithm as opposed to the object space algorithm described above. One starts with the equidistant image space coordinates (x,y) for the output image. These need to be converted to the imaging time t and slant range r. Time t serves to derive the platform position S and corresponding velocity vector $\underline{v}$ from given flight recordings.

The geometry created by the platform position S, the slant range r and known squint angle τ is the radar projection circle at the

intersection of a sphere (S,r) and a cone (S,v,τ). The intersection point(s) of circle and DEM define the object space addresses. So for each image coordinate one or more DEM addresses (X,Y,Z - coordinates) -- not grid points -- are found and interpolation takes place in the object space. The occurence of more than one intersection point happens if different terrain targets were illuminated simultaneously.
A detailed description of the image space algorithm is given in (Domik, Leberl and Raggam, 1983).

(b) Radiometric Imaging Model

The assignment of grey values to each image location is a function of the incidence angle(s) at the corresponding object space address(es). Backscatter values are modelled by standard backscatter curves (Hagfors, 1964; Muhleman, 1964) or look up tables. Shadowing is no problem for the object space algorithm, when the algorithm moves along the DEM lines from near to far range in the presorted array. An additional sorting step has to be applied in the image space algorithm to detect radar shadow. The grey values within a shadow region are set to zero.

The simulation as described above considers all of the geometric characteristics of radar imagery (foreshortening, layover, radar shadow).

The object space algorithm was applied as a fast tool with limited considerations:
(A) The flight path is approximated by a straight line at constant altitude.
(B) The ground to be imaged is represented by a digital elevation system with columns parallel to the flight path.
(C) The mesh and grid size of the DEM define the image size and resolution.

This simple method proves to be fast and applicable where special parameters need not to be studied.

A more rigorous approach is with the image space algorithm:
(A) Arbitrary flight paths and flight perturbations may be used as an input.
(B)The size of DEM and resulting image are unlimited and independent.
Also imaging in a cone (squint angle $\tau \neq 0$) as oppossed to imaging in a plane ($\tau = 0$) is possible.

Applications of radar simulation

Stereo viewability evaluation

The digital elevation model of two Greek islands, Cephalonia and Ithaca, was chosen as the height model for stereo investigations. During the SIR-A flight (Nov. 1981) these islands were imaged at two different data takes on crossing swaths. The obtained stereo pair proved to be an alternative in its quality to same side stereo.
The SIR-A radar parameters (Cimino and Elachi, 1982) were used as input parameters to the simulation, only modified in their stereo arrangements to obtain

- same side stereo / different elevation angles
- same side stereo with applied squint angle
- crossing swaths stereo / same elevation angle

A set of images was created for each of the investigations. The viewability was rated by stereoscopic viewing using hard copy images and a standard stereoscope.

Results:

Elevation angles ranging from 15 deg. to 80 deg. were used for the same side investigations. A combination of 70 deg. vs. 50 deg. elevation angle was found to be best for the Greek island elevation model and at flight altitude of 264 km (Fig. 1 and Fig. 2). The highest ranked stereo pairs are listed in Table 1.

A variation of different squint angles (τ = 0.5 deg. to 50 deg.) was applied to the best rated same side stereo image pair.
When imaging in a cone but recording the backscatter in one line the output image is geometrically and radiometrically distorted. (Fig. 3). The locations of the image pixels need to be rearranged using simple equations (see Domik et al., 1983) in an additional step to the simulation to create the geometry of imaging in a plane perpendicular to the flight velocity vector (Fig. 4). The radiometric distortions, however, increase with the squint angle, and proved to be "not acceptable" by applying squint angles of more than or equal to 30 deg.

The Greek Island SIR-A picture imaging with two tracks crossing at an angle of 34 deg. created a good stereo pair. Simulation showed that there were no stereo viewability problems up to 40 deg. of crossing angle. The viewability limit lays between 40 deg. and 42 deg.

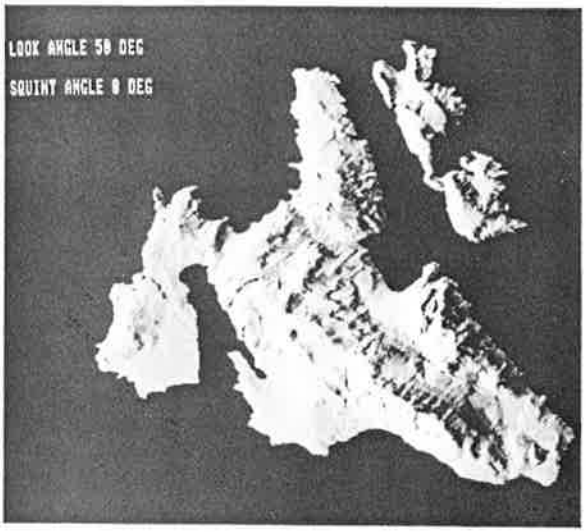

Fig. 1 : Simulated radar image : flight altitude 264 km, look angle 50 deg. off nadir, slant range presentation.

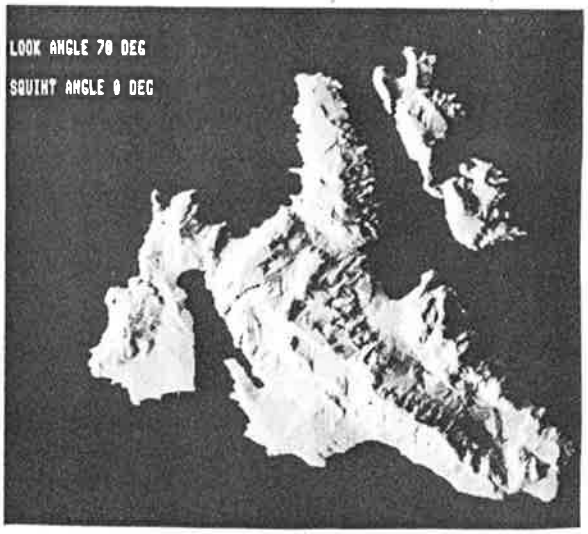

Fig. 2 : Simulated radar image : flight altitude 264 km, look angle 70 deg. off nadir, slant range presentation.

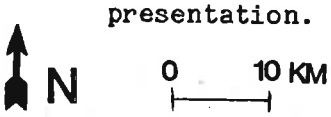

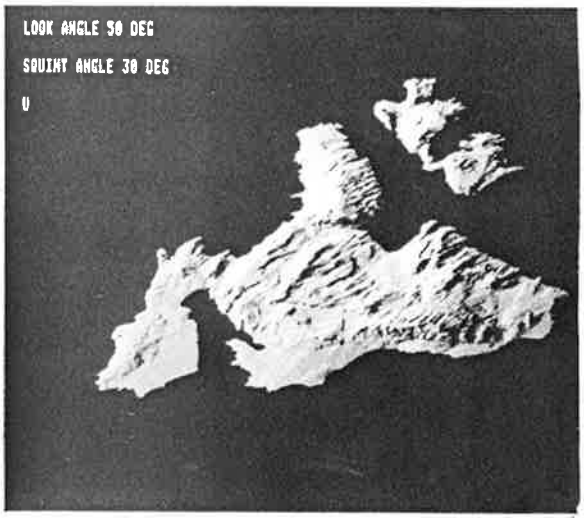

Fig. 3 : Intermediary simulation product : flight altitude 264 km, look angle 50 deg. off nadir, squint angle 30 deg., slant range presentation. Distorted geometry and radiometry.

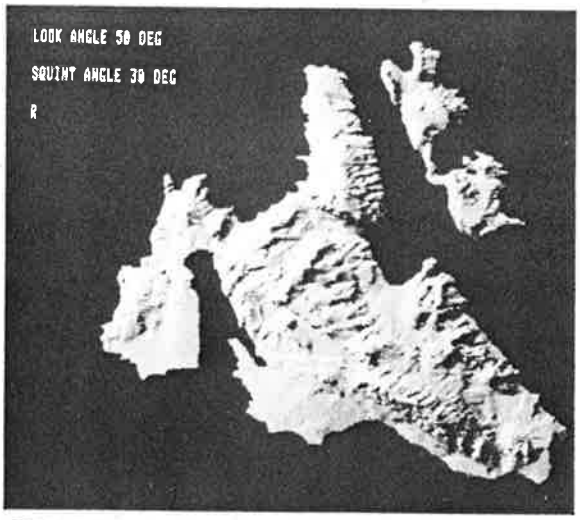

Fig. 4 : Simulated radar image : flight altitude 264 km, look angle 50 deg. off nadir, squint angle 30 deg., slant range presentation. Geometry as imaged without squint, but distorted radiometry.

RANK ORDER	ELEVATION ANGLES	INTERSECTION ANGLE
1	70^0 / 50^0	20^0
2	60^0 / 40^0	20^0
2	75^0 / 50^0	25^0
3	40^0 / 30^0	10^0
3	47^0 / 30^0	17^0
3	50^0 / 40^0	10^0
3	70^0 / 47^0	23^0
3	65^0 / 50^0	15^0

Highest ranked stereo pairs
for Greek testsite

TABLE I

Rectification

Caused by the topographic relief and its active imaging properties, radar images are distorted if compared to their photographic equivalents. For reasons of merging radar images with other data sets (e.g. LANDSAT, topo maps) rectification is an important step in radar image analysis. Caused by the radar distortions the relation of radar images to other data sets is aggrevated by the lack of visible ground control points. This is overcome by the simulation and subsequent registration of real and simulated image. Thus the relation of each image grey value to a DEM address is taken care of by the object or image space algorithm chosen as described above.
The airborne radar image in Fig. 5 (Oetztal, Austria, SAR-580 campaign; digitally processed), demonstrates the difficulty of relating radar image and corresponding DEM (Fig. 6) . Whereas the ridge in the upper part of the radar image may be identified as the ridge stretching from south-west to north-east in the DEM, it is hardly possible to find homologue points between DEM and lower part of the radar image.
Using imaging parameters and ground control points to model the flight path (Rott H., 1983 and personal communication) a simulation was performed to fit over the real image. The grey

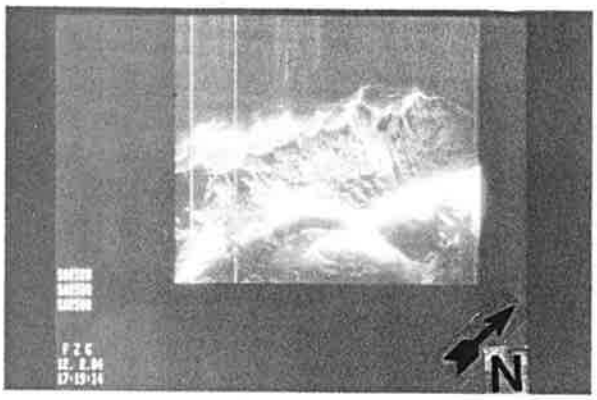

Fig. 5 : Airborne radar image (SAR-580) : X - band, HH polarisation, flight altitude 6 km; ground range presentation. Oetztal, Tyrol, Austria.

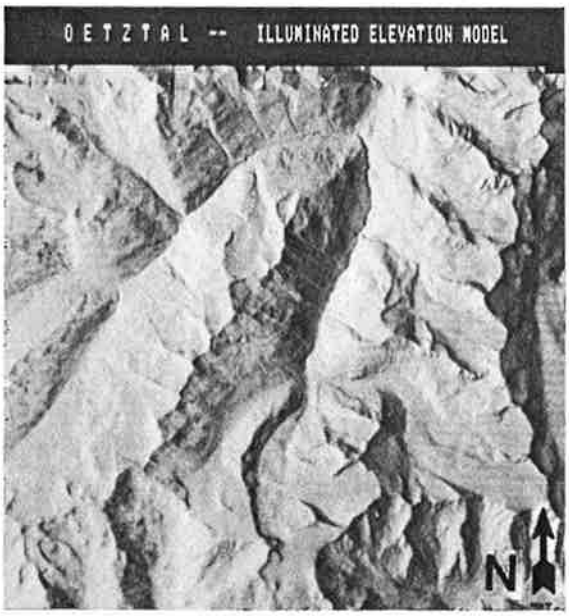

Fig. 6 : Illuminated height model of Oetztal area. Maximal elevation 3.6 km.

Fig. 7 : Simulated radar image : flight altitude 6 km, ground range presentation.

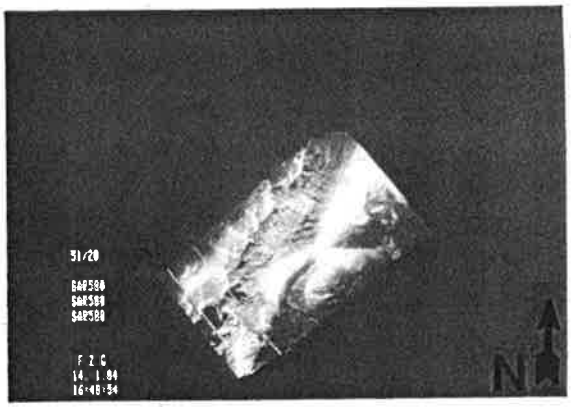

Fig. 8 : Radar ortho image : Radar grey values fit over digital elevation model.

0 1 KM

These scales do not look equal!

values were defined by a homogeneous backscatter curve dependent on the corresponding incidence angle. Between the simulation (Fig. 7) and the real image, numerous homologue points can be found, and thus a registration between real and simulated images could be performed. Differences between the two images are mainly due to errors in the roughly estimated flight path. After the registration the image grey values of the registered image are resampled at their DEM addresses (DEM addresses and image location were related through the simulation step). The ortho image in Fig. 8 shows the radar image of Fig. 5 (resolution of 24 m / pixel) fit over the topo map with a coarser resolution of 30 m / pixel of Fig. 6.

Backscatter analysis

After registering the real to the simulated image the radar grey values may be analyzed in many different aspects. The relation between the DN values and their DEM addresses is the source of the geometric rectification as described above. The relation between DN values and corresponding incidence angles proves to be a way to model backscatter curves or look up table of the radar backscatter values as a function of their incidence angle. Fig. 9 shows an area in North California as seen by SIR-A in Nov. 1981. The optically processed data were digitized and resampled to show an area of approximately 64 km square. After the simulation and additional registration step the DN values of a relatively homogenous area (indicated by the upper left box in Fig. 9) was analyzed ~~in aspects to~~ plotting their grey values vs. the incidence angle. The subsequent plot is shown in Fig. 10.

Conclusion

An elaborate simulation system for radar image analysis and radar stereo predictions has been described. The emphasis of the simulation is on a geometrically rigorous model. The current simulation contains a fast but limited program version, and a more rigorous model which allows one to select arbitrary flight paths and imaging parameters consisting of e.g. look direction, choice of slant/ground range and squint angles.

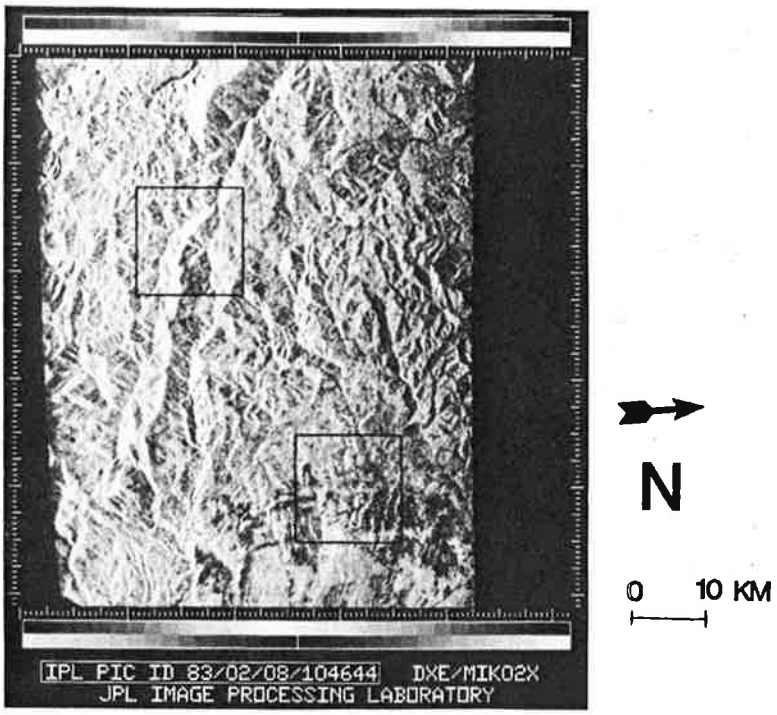

Fig. 9 : Spaceborne radar image (SIR-A) : L - band, HH polarisiation, flight altitude 265 km; slant range presentation. Northern California, USA.

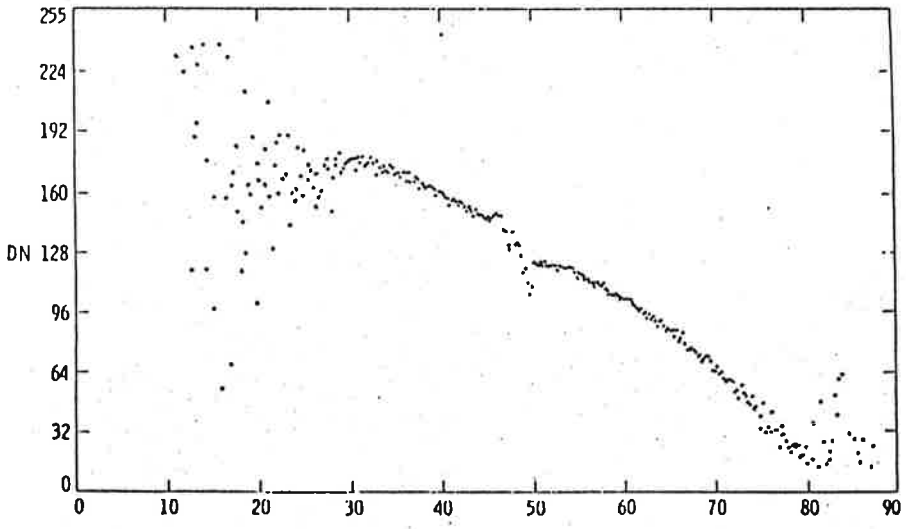

Fig. 10 : Backscatter plot : Radar DN values vs. incidence angle.

References

Cimino J. and C. Elachi, 1982:
"SIR-A Radar Parameters. ON/OFF Times. Latitude and Longitude." Internal JPL Report. Pasadena,USA.

Domik G., F. Leberl and J. Raggam, 1983:
"Evaluation of Radar Stereoscopic Viewing". DIBAG Report Nr. 11, Graz Research Center, Austria. Final report in contract Nr. F49620-82-C-0053, European Office of Aerospace and Development, London.

Domik G., F. Leberl and M. Kobrick, 1983:
"Analyse von Radarbildern mittels digitaler Hoehenmodelle". Bildmessung und Luftbildwesen, Berlin, Germany. (In print).

Hagfors T., 1964:
"Backscatter from an Undulating Surface with Applications to Radar Returns from the Moon", J. Geophys. Res. 1964, pp. 19-32.

Holtzman, J.C., V.S. Frost, J.L. Abbott and V. Kaupp, 1978:
"Radar Image Simulation". IEEE Trans. on Geoscience Electronics, Vol. GE-16.

Kaupp V., Bridges, M. Pisarek, H. MacDonald and W. Waite, 1982:
"Comparison of Simulated Stereo Radar Imagery." IGARSS '82, Munich, Paper TA4, June 1-4, 1982.

Muhleman, D.O., 1964:
"Radar Scattering from Venus and the Moon." Astronomical Journal, 69, pp. 34 - 41, 1964.

Rott H., 1983:
"SAR Data Analysis for an Alpine Test Site". Paper presented at the SAR-580 Workshop in Ispra, Italy, April 1983.